

”Density ripples” in expanding low-dimensional gases as a probe of correlations

A. Imambekov,¹ I. E. Mazets,^{2,3} D. S. Petrov,^{4,5} V. Gritsev,⁶ S. Manz,²
S. Hofferberth,⁷ T. Schumm,^{2,8} E. Demler,⁷ and J. Schmiedmayer²

¹*Department of Physics, Yale University, New Haven, Connecticut 06520, USA*

²*Atominstytut der Österreichischen Universitäten, Stadionallee 2, 1020 Vienna, Austria*

³*Ioffe Physico-Technical Institute, 194021 St.Petersburg, Russia*

⁴*Laboratoire Physique Théorique et Modèles Statistique,*

Université Paris Sud, CNRS, 91405 Orsay, France

⁵*Russian Research Center Kurchatov Institute, Kurchatov Square, 123182 Moscow, Russia*

⁶*Physics Department, University of Fribourg, Chemin du Musée 3, 1700 Fribourg, Switzerland*

⁷*Department of Physics, Harvard University, Cambridge, MA 02138, USA*

⁸*Wolfgang Pauli Institute, University of Vienna, 1090 Vienna, Austria*

(Dated: June 6, 2022)

We investigate theoretically the evolution of the two-point density correlation function of a low-dimensional ultra cold Bose gas after release from a tight transverse confinement. In the course of expansion thermal and quantum fluctuations present in the trapped systems transform into density fluctuations. For the case of free ballistic expansion relevant to current experiments, we present simple analytical relations between the spectrum of ”density ripples” and the correlation functions of the original confined systems. We analyze several physical regimes, including weakly and strongly interacting 1D Bose gases, and 2D Bose gases below the Berezinskii-Kosterlitz-Thouless (BKT) transition. For weakly interacting 1D Bose gases, we obtain an explicit analytical expression for the spectrum of density ripples which can be used for thermometry. For 2D Bose gases below the BKT transition, we show that for sufficiently long expansion times the spectrum of the density ripples has a self-similar shape, controlled only by the exponent of the first-order correlation function. This exponent can be extracted by analyzing the evolution of the spectrum of density ripples as a function of the expansion time.

PACS numbers: 03.75.Hh,67.85.-d

I. INTRODUCTION

A. Quantum noise studies of ultra cold atoms

Quantum correlations can be used to identify and study interesting novel quantum phases and regimes in ultra cold atomic systems. Recent experimental advances include detection of the Mott insulator phase of bosonic [1] and fermionic [2] atoms in optical lattices, production of correlated atom pairs in spontaneous four-wave mixing of two colliding Bose-Einstein condensates [3], studies of dephasing [4] and interference distribution functions [5] in coherently split one-dimensional atomic quasicondensates, observation of the Berezinskii-Kosterlitz-Thouless (BKT) transition [6, 7] in two-dimensional quasicondensates [8], and Hanbury-Brown-Twiss correlation measurements for non-degenerate metastable ⁴He [9] and ³He atoms [10], bosonic [11] and fermionic [12] atoms in optical lattices, and in atom lasers [13]. In one-dimensional atomic gases [14, 15, 16, 17], in situ measurements of correlations have been attained by means of photoassociation spectroscopy [18] or by measuring the three-body inelastic decay [19], using the proportionality of the corresponding rates to the zero-distance two-particle and three-particle correlation functions, respectively [20].

Recently it was demonstrated that one can detect single neutral atoms in a tight trap or guide [21, 22, 23, 24,

25, 26]. However, direct (not inferred from any kind of atomic loss rate [18, 19]) observation of interatomic correlations at short distances in trapped ultra cold atomic gases is hindered in many cases by either the finite spatial resolution of the optical detection technique or the very low detection efficiency of the scanning electron microscope [24].

In this paper we address the question of how the correlations in the low-dimensional system evolve during the time-of-flight expansion, and discuss how the density variations in the time-of-flight images relate to the properties of the original trapped quantum gas. These ”density ripples” in the expanding gas reflect the original thermal or quantum phase fluctuations existing in the cloud under confinement. Such phase fluctuations are already present in 3D Bose condensed clouds under an external confinement with large aspect ratio [27]. Their effect on density ripples of expanding clouds has been observed [28, 29, 30], but quantitative analysis of such experiments was complicated, since one had to take into account interactions in the course of expansion. However, for sufficiently strong transverse confinement reached in current experiments with low-dimensional gases (chemical potential of the order of the transverse confinement frequency), the gas expands rapidly in the transverse direction, so interactions during the expansion stage can be safely neglected. Then one can develop a simple analytical theory, which directly relates the spectrum of the density ripples after the expansion to the correlation

functions of the original fluctuating condensates.

B. Density ripples in expanding condensates. Preview

We consider one- or two-dimensional atomic gases released from a tight trap formed by a scalar potential as realized on atom chips or in optical lattice experiments. We consider the situation when free expansion takes place in all three dimensions.

This should be contrasted to the expansion of such a gas inside a waveguide [16, 31, 32, 33, 34, 35, 36, 37, 38, 39], with the transverse confinement being permanently maintained. In the latter case, the nonlinear atomic coupling constant

$$g_{1D} = 2\hbar\omega_{\perp}a_s, \quad (1)$$

where ω_{\perp} is the transverse trapping frequency and a_s is the atomic s -wave scattering length, remains the same. While a bosonic gas rarifies during such expansion, collisions remain important. For example, in the 1D case dynamics asymptotically reaches the limiting Tonks-Girardeau [40] regime of impenetrable bosons.

In our case, if the fundamental frequency of the potential of the transverse confinement is much larger than the initial chemical potential μ or the temperature of the atoms ($\mu, k_B T \ll \hbar\omega_{\perp}$), the expansion in the transverse directions is determined mainly by the kinetic energy stored in the initial localized state of the transverse motion. Interatomic collisions play almost no role in the expansion. Moreover tight transverse confinement decouples the motion of trapped atoms in the longitudinal and transverse directions. Thus when analyzing density ripples we can reduce the problem to the same number of dimensions as the initial trap (see discussion below in Sec. II). For a 1D trap we consider a one-dimensional spectrum of density ripples, and for atoms which were originally confined in a pancake trap we analyze two-dimensional density ripples.

Before we consider a general formalism, it is useful to present the analysis for the simplest situation. Let us assume that the initial state can be described using the mean-field Bogoliubov approach [41, 42, 43]. Let $\hat{\Psi}_{\vec{k}}$ be the creation operator of atoms at momentum \vec{k} right before the expansion. After free expansion during time t , in the Heisenberg representation we have $\hat{\Psi}_{\vec{k}}^{\dagger}(t) = \hat{\Psi}_{\vec{k}}^{\dagger} e^{i\frac{\hbar^2 k^2 t}{2m}}$, where m is the atomic mass. Then the density operator at time t is given by

$$\rho(\vec{r}, t) = \frac{1}{L} \sum_{\vec{k}_1, \vec{k}_2} \hat{\Psi}_{\vec{k}_1}^{\dagger} \hat{\Psi}_{\vec{k}_2} e^{-i(\vec{k}_1 - \vec{k}_2)\vec{r}} e^{i\frac{\hbar^2}{2m}(k_1^2 - k_2^2)}, \quad (2)$$

and for the density correlation function we obtain

$$\langle \rho(\vec{r}_1, t) \rho(\vec{r}_2, t) \rangle = \frac{1}{L^2} \sum_{\vec{k}_1, \vec{k}_2, \vec{k}_3, \vec{k}_4} \langle \hat{\Psi}_{\vec{k}_1}^{\dagger} \hat{\Psi}_{\vec{k}_2} \hat{\Psi}_{\vec{k}_3}^{\dagger} \hat{\Psi}_{\vec{k}_4} \rangle$$

$$\times e^{-i(\vec{k}_1 - \vec{k}_2)\vec{r}_1} e^{-i(\vec{k}_3 - \vec{k}_4)\vec{r}_2} e^{i\frac{\hbar^2}{2m}(k_1^2 - k_2^2)} e^{i\frac{\hbar^2}{2m}(k_3^2 - k_4^2)}. \quad (3)$$

The expectation value $\langle \hat{\Psi}_{\vec{k}_1}^{\dagger} \hat{\Psi}_{\vec{k}_2} \hat{\Psi}_{\vec{k}_3}^{\dagger} \hat{\Psi}_{\vec{k}_4} \rangle$ should be taken in the original condensate before the expansion. Within the mean-field Bogoliubov theory only a state with $k = 0$ is macroscopically occupied. Thus in Eq. (3) we take two operators to be $\sqrt{N} = \sqrt{n_{1D}L}$, where n_{1D} is the atomic density before the expansion. Then Eq. (3) can be written as

$$\langle \rho(\vec{r}_1, t) \rho(\vec{r}_2, t) \rangle = n_{1D}^2 + \frac{n_{1D}}{L} \sum_{\vec{q} \neq 0} e^{i\vec{q}(\vec{r}_1 - \vec{r}_2)} \left[1 + 2\langle \hat{\Psi}_{\vec{q}}^{\dagger} \hat{\Psi}_{\vec{q}} \rangle + \left(\langle \hat{\Psi}_{-\vec{q}} \hat{\Psi}_{\vec{q}} \rangle + \langle \hat{\Psi}_{-\vec{q}}^{\dagger} \hat{\Psi}_{\vec{q}}^{\dagger} \rangle \right) \cos \frac{\hbar^2 q^2 t}{m} \right]. \quad (4)$$

The Bogoliubov theory predicts expectation values of $\langle \hat{\Psi}_{-\vec{q}} \hat{\Psi}_{\vec{q}} \rangle$, $\langle \hat{\Psi}_{-\vec{q}}^{\dagger} \hat{\Psi}_{\vec{q}}^{\dagger} \rangle$, and $1 + 2\langle \hat{\Psi}_{\vec{q}}^{\dagger} \hat{\Psi}_{\vec{q}} \rangle$ as

$$\langle \hat{\Psi}_{-\vec{q}} \hat{\Psi}_{\vec{q}} \rangle = \langle \hat{\Psi}_{-\vec{q}}^{\dagger} \hat{\Psi}_{\vec{q}}^{\dagger} \rangle = -\frac{\mu}{2E_q} \left[1 + 2n_B \left(\frac{E_q}{k_B T} \right) \right], \quad (5)$$

$$1 + 2\langle \hat{\Psi}_{\vec{q}}^{\dagger} \hat{\Psi}_{\vec{q}} \rangle = \frac{\epsilon_q + \mu}{E_q} \left[1 + 2n_B \left(\frac{E_q}{k_B T} \right) \right], \quad (6)$$

where $\epsilon_q = \hbar^2 q^2 / (2m)$, $\mu = g_{1D} n_{1D}$ is the chemical potential, $E_q = \sqrt{\epsilon_q(2\mu + \epsilon_q)}$ is the Bogoliubov excitation spectrum, and n_B is the Bose occupation number.

From these equations we can easily find the mean-field spectrum of density ripples $\langle |\rho^{MF}(q, t)|^2 \rangle$ (see Eq. (21) and the discussion nearby for the precise mathematical definition of the spectrum)

$$\langle |\rho^{MF}(q, t)|^2 \rangle = n_{1D} \left[1 + 2n_B \left(\frac{E_q}{k_B T} \right) \right] \times \left[\frac{\epsilon_q}{E_q} + \frac{\mu}{E_q} \left(1 - \cos \frac{\hbar^2 q^2 t}{m} \right) \right]. \quad (7)$$

The general character of the spectrum is clear from Eq. (7). As a function of momentum it is not monotonic. We find minima near $\hbar q^2 t / m = 2\pi n$, and maxima close to $\hbar q^2 t / m = \pi(2n - 1)$, where n is a positive integer number. Note that while the positions of maxima and minima are essentially universal, the amplitude of individual maxima depends on both temperature and interaction strength.

The mean-field analysis leading to Eq. (7) is conceptually simple but has limited applicability. It is applicable for weakly interacting 3D Bose condensates if the interactions during expansion are switched off using Feshbach resonances [44]. In lower dimensions, thermal and quantum phase fluctuations are expected to suppress true long range order in 2D Bose condensates at finite temperature [45] and in 1D Bose condensates even at zero temperature [46]. In this paper we show how analysis of the density ripples can be extended to more complicated but experimentally relevant situations when the mean-field approach breaks down. We will find a similar structure

to Eq. (7): positions of maxima and minima of the spectrum are given by the same approximate universal conditions on the momenta. However, explicit expressions for the strength of individual maxima will be very different. They will contain rich information about fluctuations of low-dimensional condensates.

C. Relation to other work

Conceptually, the question we consider in this paper is somewhat similar to the interpretation of cosmological observations. In the latter case, quantum fluctuations present in the early Universe after its expansion result in observable anisotropies of the cosmic microwave background radiation [47, 48], and in the density ripples of matter which eventually evolve into galaxies [49]. In our case, density ripples of the expanding clouds contain important information about correlations present in the trapped state.

In addition to the mentioned approaches, several other techniques have been used to experimentally study correlations of low-dimensional and highly elongated 3D gases. Some of them rely on creation of two copies of the same cloud [50, 51, 52, 53, 54], while others require analysis of noise correlations [55] or in situ density fluctuation statistics [56]. Interference experiments between two low-dimensional clouds [4, 5, 8] can also be used to characterize two-point and multi-point correlation functions [57, 58, 59, 60]. Analysis of density ripples is a much simpler experiment and, as we discuss in this paper, can be used for thermometry. This is particularly important for weakly interacting 1D Bose quasicondensates [61, 62], for which the standard approach to measuring temperature by fitting density profiles cannot be extended to temperatures of the order of the chemical potential. In this regime, the chemical potential is very weakly dependent on the temperature [63], thus finite temperature leads only to small corrections to the "inverted parabola" density profile [64].

On the theoretical side, there has recently been significant interest in correlation functions of the 1D Bose gas. At distances much larger than the healing length, correlation functions are described by Luttinger liquid theory [65, 66, 67]. In the weakly interacting quasicondensate regime, correlation functions can be described by extension of Bogoliubov theory to low-dimensional gases [62, 63, 68, 69, 70]. In the strongly interacting regime, one can use "fermionization" [40] of a 1D Bose gas to evaluate correlation functions at all distances as certain determinants [71]. The Lieb-Liniger model [72] which describes the 1D Bose gas is exactly solvable, and one can also analytically obtain zero-distance two-point [73] and three-point [74] density correlations for any interaction strength, and extract certain dynamical correlation functions [75, 76, 77, 78, 79] from the exact solution. Various numerical techniques have been used as well [64, 80, 81], and recent results including the decoher-

ent quantum regime [82] are summarized in Refs. [83, 84].

Two-dimensional systems have also been a subject of considerable experimental [8, 15, 54, 85, 86, 87, 88] and theoretical work [61, 70, 89, 90, 91, 92, 93, 94, 95, 96, 97].

D. Structure of the paper

This paper is organized as follows. In Sec. II we derive simple analytical relations between the density ripples after the expansion and the correlation functions of the original system before the expansion. In Sec. III A we analyze the case of weakly interacting 1D Bose gases and obtain explicit expression for the spectrum of density ripples. In Sec. III B we consider the case of a strongly interacting 1D Bose gas. In Sec. III C we review general features of the density-density correlation function in expanding 1D Bose clouds. In Sec. IV we discuss 2D Bose systems below the BKT transition [6, 7]. We summarize our results and make concluding remarks in Sec. V.

II. FREE EXPANSION

In this section we focus on the atoms expanding from a one-dimensional trap. The atom field operator evolution during the free expansion is given by [98]

$$\hat{\Psi}(\mathbf{r}, t) = \int d^3\mathbf{r}' G_3(\mathbf{r} - \mathbf{r}', t) \hat{\Psi}(\mathbf{r}', 0), \quad (8)$$

where the Green's function of free motion is

$$G_3(\mathbf{r} - \mathbf{r}', t) = G_1(x - x', t) G_1(y - y', t) G_1(z - z', t), \quad (9)$$

$$G_1(\xi, t) = \sqrt{\frac{m}{2\pi i \hbar t}} \exp\left(i \frac{m\xi^2}{2\hbar t}\right), \quad (10)$$

m being the atomic mass. Tight transverse confinement decouples the motion of trapped atoms in the (y, z) -plane and along the waveguide axis x , so that the transverse motion is confined to its ground state $f_{\perp}(y, z)$, and $\hat{\Psi}(\mathbf{r}, 0) = f_{\perp}(y, z) \hat{\psi}(x, 0)$. This, alongside with Eq. (9), allows for a separation of motion in the longitudinal and transverse directions, effectively reducing the problem to 1D.

We introduce the two-particle density matrix for the longitudinal motion as

$$\rho(x_1, x_2; x'_1, x'_2; t) = \left\langle \hat{\psi}^{\dagger}(x'_1, t) \hat{\psi}^{\dagger}(x'_2, t) \hat{\psi}(x_2, t) \hat{\psi}(x_1, t) \right\rangle. \quad (11)$$

Then we define the two-point density correlation function

$$g_2(x_1, x_2; t) = \frac{\rho(x_1, x_2; x_1, x_2; t)}{n(x_1, t)n(x_2, t)}, \quad (12)$$

where $n(x, t) = \left\langle \hat{\psi}^{\dagger}(x, t) \hat{\psi}(x, t) \right\rangle$. The free evolution of the two-particle density matrix is given by a convolution

of the two-particle density matrix at $t = 0$ with four respective Green's functions, one for each spatial argument, two of the Green's functions being complex conjugate. We are interested in the case $x_1 = x'_1$ and $x_2 = x'_2$ in the final state. Then we obtain

$$\begin{aligned} \rho(x_1, x_2; x_1, x_2; t) = & \\ \int dx_3 \int dx'_3 \int dx_4 \int dx'_4 & G_1(x_1 - x_3, t) G_1(x_2 - x_4, t) \\ \times G_1^*(x_1 - x'_3, t) G_1^*(x_2 - x'_4, t) & \rho(x_3, x_4; x'_3, x'_4; 0). \end{aligned} \quad (13)$$

We assume that the product of the typical velocity of the atoms in the x -direction and the expansion time is much smaller than the size of the trapped atomic cloud. Then we are allowed to consider a uniform sample with length $L \rightarrow \infty$, with the 1D number density $n_{1D} = N/L$ being kept constant in the thermodynamic limit (N being the total number of atoms). Note that this limit is opposite to the conventional limit of infinitely large expansion times, in which density in real space reflects the initial momentum distribution (in that regime, it was recently proposed [99] that noise correlations in density profiles can be used to probe properties of low-dimensional gases).

In our limit $n(x, t) = n_{1D}$ is constant in time, and the two-particle density matrix is translationally invariant (it does not change if all four of its spatial arguments are shifted by the same amount) at any time. The density correlation function then depends on the coordinate difference only, so we use the notation

$$g_2(x_1 - x_2; t) \equiv g_2(x_1, x_2; t). \quad (14)$$

Using the translational invariance of the two-particle density matrix and the identity

$$\delta(x) = \frac{1}{2\pi} \int_{-\infty}^{\infty} dy \exp(iyx), \quad (15)$$

we arrive at

$$\begin{aligned} \rho(x_1 - x_2; x_1 - x_2; t) = & \frac{m}{4\pi\hbar t} \\ \times \int_{-\infty}^{\infty} dx \int_{-\infty}^{\infty} dx' \exp \left\{ i \frac{m}{4\hbar t} \left[(x_1 - x_2 - x)^2 \right. \right. & \\ \left. \left. - (x_1 - x_2 - x')^2 \right] \right\} \rho(x; x'; 0), & \end{aligned} \quad (16)$$

where

$$\rho(x; x'; t) \equiv \rho \left(\frac{x}{2}, -\frac{x}{2}; \frac{x'}{2}, -\frac{x'}{2}; t \right). \quad (17)$$

Obviously, $\rho(x_1, x_2; x_1, x_2; t) = \rho(x_1 - x_2; x_1 - x_2; t) = n_{1D}^2 g_2(x_1 - x_2; t)$. The physical meaning of Eq. (16) is that the motion of the center of mass of an atomic pair plays no role in the dynamics of establishing $g_2(x_1 - x_2; t)$, which is fully determined by the relative motion. The relative-motion degree of freedom is characterized by the reduced mass $m/2$ [100].

Let us now consider some properties of the two-particle density matrix $\varrho(x_1; x_2; t)$ for bosons. Changing the sign of x_1 or x_2 is equivalent to a permutation of two bosons and, hence, does not change the two-particle density matrix, i.e.,

$$\varrho(x_1; x_2; t) = \varrho(|x_1|; |x_2|; t). \quad (18)$$

For the regimes we consider the density matrix of neutral bosons can be assumed to be real. This, together with the hermiticity property, results in

$$\varrho(x_1; x_2; t) = \varrho(x_2; x_1; t). \quad (19)$$

Using Eqs. (18, 19) and Fourier transforming the Green's functions, we can reduce Eq. (16) to

$$\begin{aligned} \varrho(x; x; t) = & \frac{2}{\pi} \int_0^{\infty} dq \int_0^{\infty} dX \cos qx \cos qX \\ & \times \varrho \left(\left| X - \frac{\hbar qt}{m} \right|; \left| X + \frac{\hbar qt}{m} \right|; 0 \right). \end{aligned} \quad (20)$$

Alternatively, this equation can be written as

$$\begin{aligned} \langle |\rho(q, t)|^2 \rangle = & \int_{-\infty}^{\infty} dX \cos qX \\ & \times \left\langle \hat{\psi}^\dagger \left(\frac{\hbar qt}{m}, 0 \right) \hat{\psi}^\dagger(X, 0) \hat{\psi} \left(X + \frac{\hbar qt}{m}, 0 \right) \hat{\psi}(0, 0) \right\rangle. \end{aligned} \quad (21)$$

Here $\langle |\rho(q, t)|^2 \rangle$ is the spectrum of density ripples at time t , which in experiment can be obtained by Fourier transforming absorption images after expansion [101]. It is related to two-point density correlation function as [102]

$$\langle |\rho(q, t)|^2 \rangle = n_{1D}^2 \int_{-\infty}^{\infty} dx \exp(iqx) (g_2(x; t) - 1). \quad (22)$$

Equations (20) and (21) provide a simple analytical relation between the properties of the density ripples after the expansion and the correlation functions before the expansion.

It is straightforward to generalize the above analysis to the 2D case. In particular, the analog of Eq. (21) for the time evolution of the two-point density correlation function has the same form, with X substituted by \mathbf{r} and q treated as a 2D vector. Namely, we obtain

$$\begin{aligned} \langle |\rho(\mathbf{q}, t)|^2 \rangle = & \int_{R^2} d^2\mathbf{r} \cos \mathbf{q}\mathbf{r} \\ & \times \left\langle \hat{\psi}^\dagger \left(\frac{\hbar \mathbf{q}t}{m}, 0 \right) \hat{\psi}^\dagger(\mathbf{r}, 0) \hat{\psi} \left(\mathbf{r} + \frac{\hbar \mathbf{q}t}{m}, 0 \right) \hat{\psi}(0, 0) \right\rangle. \end{aligned} \quad (23)$$

III. 1D BOSE GASES

A. Weakly interacting 1D Bose gases

In this subsection we will consider the spectrum of density ripples of weakly interacting 1D quasicondensates. Before we proceed to full analytical theory, let us return to the simple mean-field Bogoliubov approach, which we

discussed in the introduction. Readers may be sceptical about the applicability of the mean-field approach to 1D. Indeed, there is no long-range order for 1D gases even at zero temperature [46], and the mean-field approach is generally not applicable. However, in the regime of weak interactions and under certain conditions on the expansion time t , the spectrum of density ripples is captured correctly by the mean-field approach, as we will verify later in a rigorous calculation.

We consider Eq. (7) in the limit $\epsilon_q \ll \mu$, $E_q \ll k_B T$. In this case one can neglect the first term in the second parentheses, use an approximation $E_q \propto q$, and expand the Bose occupation number, leading to

$$\frac{\langle |\rho^{MF}(q, t)|^2 \rangle}{n_{1D}^2} \approx \frac{2mk_B T \left(1 - \cos \frac{\hbar^2 q^2 t}{m}\right)}{\hbar^2 n_{1D} q^2}. \quad (24)$$

Let us now present a full calculation, which doesn't make a mean-field approximation. For weak interactions Bogoliubov theory has been extended to low-dimensional quasicondensates [63], and can be used to calculate correlation functions at all distances. For quasicondensates, the fluctuations of the phase are described by the Gaussian action. For Gaussian actions, higher order correlation functions are simply related to two-point correlation functions (see e.g. Refs. [103, 104]), and the four-point correlation function in Eq. (21) factorizes into products of two-point correlation functions of bosonic fields as

$$\frac{\langle \hat{\psi}^\dagger(x'_1, 0) \hat{\psi}^\dagger(x'_2, 0) \hat{\psi}(x_1, 0) \hat{\psi}(x_2, 0) \rangle}{\langle \hat{\psi}^\dagger(x'_1, 0) \hat{\psi}(x'_2, 0) \rangle \langle \hat{\psi}^\dagger(x_1, 0) \hat{\psi}(x_2, 0) \rangle} = \frac{\prod_{i,j=1}^2 \langle \hat{\psi}^\dagger(x'_i, 0) \hat{\psi}(x_j, 0) \rangle}{\langle \hat{\psi}^\dagger(x'_1, 0) \hat{\psi}(x'_2, 0) \rangle \langle \hat{\psi}^\dagger(x_1, 0) \hat{\psi}(x_2, 0) \rangle}. \quad (25)$$

The two-point correlation function $\langle \hat{\psi}^\dagger(x'_1, 0) \hat{\psi}(x_1, 0) \rangle = n_{1D} g_1(x'_1 - x_1)$ is translationally invariant, and is simply related to predictions of the Bogoliubov theory. For 1D quasicondensates, one has [63]

$$g_1(x) = \frac{\langle \hat{\psi}^\dagger(x, 0) \hat{\psi}(0, 0) \rangle}{n_{1D}} = \exp \left[-\frac{1}{2K} f \left(\frac{x}{\xi_h} \right) \right], \quad (26)$$

where $K = \pi \hbar n_{1D} / (mc) \gg 1$ is the Luttinger liquid parameter, c is the speed of sound, $\xi_h = \hbar / \sqrt{m\mu}$ is the healing length, and μ is the chemical potential. When only the lowest transverse mode is occupied ($\mu \ll \hbar \omega_\perp$), speed of sound is given by $c = \sqrt{2\hbar \omega_\perp n_{1D} a_s / m}$. The dimensionless function $f(s)$ depends on the temperature, and equals

$$f(s) = 2 \int_0^\infty dk (1 - \cos ks) \{ [u_k^2 + v_k^2] n_k + v_k^2 \}, \quad (27)$$

where

$$u_k = \frac{1}{2} \left[\left(\frac{k^2 + 4}{k^2} \right)^{1/4} + \left(\frac{k^2}{k^2 + 4} \right)^{1/4} \right], \quad (28)$$

$$v_k = \frac{1}{2} \left[\left(\frac{k^2}{k^2 + 4} \right)^{1/4} - \left(\frac{k^2 + 4}{k^2} \right)^{1/4} \right], \quad (29)$$

$$n_k = \frac{1}{\exp \left(\frac{\mu \sqrt{k^2(k^2+4)}}{2k_B T} \right) - 1}. \quad (30)$$

For finite temperatures, the function $f(s)$ has the following asymptotic behavior

$$f(s) \approx \pi |s| \frac{k_B T}{\mu} + C \text{ for } \pi |s| \frac{k_B T}{\mu} \gg 1, \quad (31)$$

where $C \equiv C(k_B T / \mu)$ is of order $O(1)$ for $k_B T \sim \mu$.

Quasicondensate theory is valid [63, 83, 84] for temperatures

$$k_B T / \mu \ll K / \pi, \quad (32)$$

significantly beyond the regime of validity of Luttinger liquid theory, which is restricted to $k_B T / \mu \ll 1$. The longitudinal density profile of a quasicondensate in external harmonic confinement follow the "inverted parabola" shape under condition (32), see e.g. Ref. [64]. Due to the low fraction of the thermally populated excited states, it is problematic to extract the temperature of the gas from fitting bimodal distributions to the observed density profiles. Below we show that the spectrum of density ripples can be used as a convenient tool to characterize the temperature, and is sensitive to temperatures of the order of the chemical potential.

To be specific, let us consider the case of ^{87}Rb atoms (scattering length $a_s = 5.2 \text{ nm}$) with density $n_{1D} = 40 \mu\text{m}^{-1}$ and transverse confinement frequency $\omega_\perp = 2\pi \times 2 \text{ kHz}$, resulting in Luttinger liquid parameter $K \approx 47$ and healing length $\xi_h \approx 0.37 \mu\text{m}$. We can use Eqs. (25)-(30) to numerically evaluate in-trap correlation functions. By performing then a numerical integration of Eq. (21) for various temperatures and expansion times, we can evaluate the spectrum of density ripples under condition (32), and the results are shown in Figs. 1 and 2. In the inset to Fig. 2 we also show $g_2(x; t)$ evaluated using the inverse of Eq. (22). In the quasicondensate regime the behavior of $g_2(x; t)$ follows the qualitative discussion of Sec. III C.

There are several qualitative features that should be noted. The spectrum of density ripples is not a monotonic function, and can also have several maxima. The positions of the maxima only weakly depend on the temperature, and are mostly determined by the expansion time. The amplitude of the ripples, on the other hand, significantly depends both on the expansion time and temperature.

Let us now derive a simple analytical expression for the spectrum of density ripples, which is valid in the regime (justified below after Eq. (39))

$$\frac{\pi}{\xi_h} \sqrt{\frac{\hbar t}{m}} \frac{k_B T}{\mu} \gg 1. \quad (33)$$

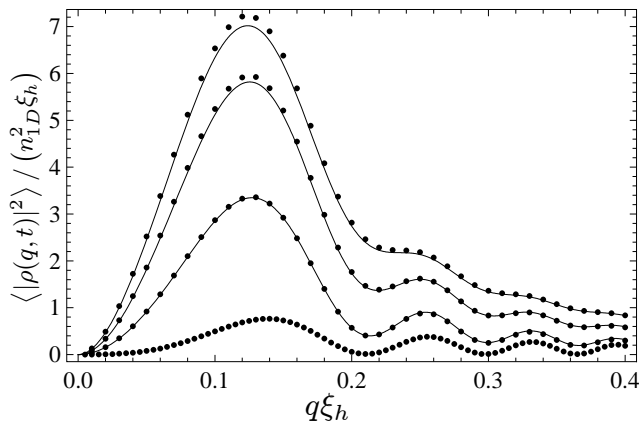


FIG. 1: Normalized spectrum of density ripples $\langle |\rho(q, t)|^2 \rangle / (n_{1D}^2 \xi_h)$ for weakly interacting 1D quasicondensate of ^{87}Rb atoms with density $n_{1D} = 40 \mu\text{m}^{-1}$, transverse confinement frequency $\omega_{\perp} = 2\pi \times 2 \text{ kHz}$, Luttinger liquid parameter $K \approx 47$, and healing length $\xi_h \approx 0.37 \mu\text{m}$. Expansion time is fixed at $t = 27 \text{ ms}$ (with $\frac{1}{\xi_h} \sqrt{\frac{\hbar t}{m}} \approx 11.8$), and temperatures equal (top to bottom) $T = 40 \text{ nK}$ ($k_B T / \mu = 1$), $T = 27 \text{ nK}$ ($k_B T / \mu = 0.67$), $T = 12 \text{ nK}$ ($k_B T / \mu = 0.3$), and $T = 0$. Values on the axes of this and subsequent plots are dimensionless. Dots are obtained by numerical integration of Eq. (21) in the weakly interacting limit making use of Eqs. (25)-(30). Solid lines correspond to analytical results (37), which are derived under condition (33).

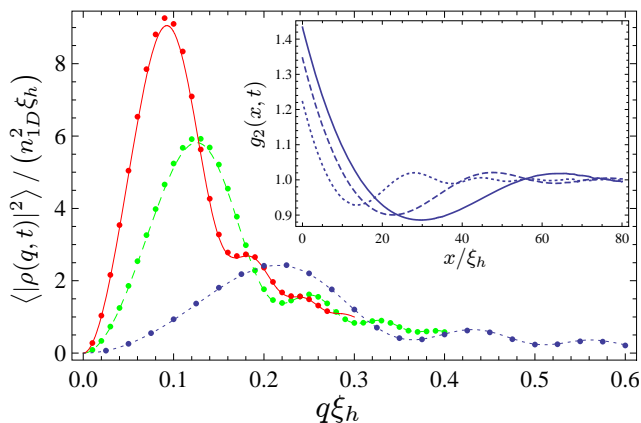


FIG. 2: (Color Online) Normalized spectrum of density ripples $\langle |\rho(q, t)|^2 \rangle / (n_{1D}^2 \xi_h)$ with the same parameters as in Fig. 1 but for a fixed temperature $T = 27 \text{ nK}$ ($k_B T / \mu = 0.67$), and various times of flight: $t = 49 \text{ ms}$ (red, solid), $t = 27 \text{ ms}$ (green, dashed), and $t = 9.5 \text{ ms}$ (blue, dotted). Dots are obtained by numerical integration of Eq. (21) in the weakly interacting limit making use of Eqs. (25)-(30). Lines correspond to analytical results (37), which are derived under condition (33). Inset shows $g_2(x, t)$, obtained from $\langle |\rho(q, t)|^2 \rangle$ using the inverse of Eq. (22).

Under this condition one can use Eq. (31) and approximate the two-point correlation function by

$$g_1(x) \approx \exp(-|x|/\lambda_T) \text{ for } |x| \gg \xi_h \frac{\mu}{k_B T}, \quad (34)$$

where λ_T is defined by

$$\lambda_T = \frac{2K\xi_h\mu}{\pi k_B T} = \frac{2\hbar^2 n_{1D}}{mk_B T}, \quad (35)$$

and does not depend on interaction strength, as long as Eq. (32) is satisfied.

Using Eqs. (25) and (34), the second line of Eq. (21) can be written as

$$\frac{g_1(\hbar qt/m)^2 g_1(X)^2}{g_1(X - \hbar qt/m) g_1(X + \hbar qt/m)} \approx \exp\left(\frac{-X}{\lambda_T}\right) \text{ for } X \leq \frac{\hbar qt}{m},$$

and $\exp\left(\frac{-\hbar qt}{m\lambda_T}\right)$ otherwise.

The constant term $\exp\left(\frac{-\hbar qt}{m\lambda_T}\right)$ is responsible for $g_2(x \rightarrow \infty, t) = 1$. Since according to Eq. (21) we need to take a Fourier transform of the above expression, subtracting the constant on the whole interval $(0, \infty)$ doesn't affect $\langle |\rho(q, t)|^2 \rangle$ for $q \neq 0$, and we obtain

$$\frac{\langle |\rho(q, t)|^2 \rangle}{n_{1D}^2} \approx 2 \int_0^{\frac{\hbar qt}{m}} dx \cos qx \left(\exp\left(\frac{-x}{\lambda_T}\right) - \exp\left(\frac{-\hbar qt}{m\lambda_T}\right) \right). \quad (36)$$

This integral can be evaluated in a closed form, and leads to an analytical answer

$$\frac{\langle |\rho(q, t)|^2 \rangle}{n_{1D}^2 \xi_h} \approx \frac{\lambda_T q - e^{-\frac{2\hbar qt}{m\lambda_T}} \left(\lambda_T q \cos \frac{\hbar q^2 t}{m} + 2 \sin \frac{\hbar q^2 t}{m} \right)}{q \xi_h (1 + \lambda_T^2 q^2)}. \quad (37)$$

Note that the last equation reduces to Eq. (24) when $\lambda_T q \gg 1$ and $\hbar qt/m\lambda_T \ll 1$. Figs. 1 and 2 show an excellent agreement between the analytical result and numerical integration described earlier after Eq. (32). The analytical result shows the same non-monotonic behaviour as the numerical calculations. The parameter λ_T defines a timescale

$$t_c \approx 6.5 \frac{m\lambda_T^2}{\hbar} \quad (38)$$

after which only a single maximum persists. When several maxima and minima are present, their positions can be estimated by

$$\frac{\hbar q^2 t}{m} \approx \pi(2n - 1/2 \mp 1/2), \quad (39)$$

where the upper (lower) sign corresponds to the n -th maximum (minimum). These conditions can be understood as a "standing wave" conditions in Eq. (36), and become more precise at lower temperatures.

The appearance of minima and maxima in the spectrum of density ripples can be understood in terms of

matter-wave near field diffraction. The analogous effect for light waves (in the spatial domain) is known as the Talbot effect [105]. Its matter-wave counterpart has been also observed in diffraction of atoms on a grating [106]. In our case, we observe near-field diffraction in the time domain. For each expansion time, a certain momentum contribution will be "imaged" onto itself, leading to a minimum in the spectrum of density ripples for a given momentum q . As compared to diffraction on a regular grating with a fixed period, the typical fluctuation length in the trapped cloud is not constant, but distributed around the thermal length λ_T . Therefore, minima in the spectrum appear for any sufficiently small expansion time, according to condition (39).

The condition (33) can now be justified in the regime where $\langle |\rho(q, t)|^2 \rangle$ is near its largest values. In such case most of the contributions to Eq. (21) come from distances of the order $\sqrt{\hbar t/m}$, and Eq. (33) follows from Eq. (32).

So far we have been assuming that the quasicondensate is deep in the 1D regime, $\mu, k_B T \ll \hbar\omega_\perp$. While Eqs. (25)-(30) are valid only under such assumption, Eqs. (34) and (35) also work in the weakly interacting quasi-1D regime,

$$\mu, k_B T \sim \hbar\omega_\perp. \quad (40)$$

Indeed, they rely only on the 1D nature of long range correlations, weakness of interactions, and the property $cK = \pi n_{1D}/m$, which is a consequence of the Galilean invariance [66]. In Eqs. (32) and (33), the Luttinger liquid parameter K can be obtained as $K = \hbar\pi n_{1D}/(mc)$, where the square of the sound velocity c can be determined from compressibility as $c^2 = n_{1D}(\partial\mu/\partial n_{1D})/m$. For chemical potential μ , one can use an approximate relation [107] $\mu = \hbar\omega_\perp(\sqrt{1 + 4a_s n_{1D}} - 1)$.

Let us now briefly review the conditions under which one can neglect interactions in expanding 1D clouds and the effects of finite condensate length L . Transverse expansion takes place at the times of the order of inverse transverse confinement ω_\perp^{-1} . Up to the times of this order, one cannot neglect interactions during the expansion. Correlation functions which enter Eq. (21) will be smeared up to the distances of the order $\delta x \sim c/\omega_\perp = \xi_h \mu/\omega_\perp$, and smearing will only weakly affect the final result for $\langle |\rho(q, t)|^2 \rangle$ if $q\delta x \ll 1$. Thus to observe an oscillating spectrum of density ripples, one needs to satisfy the condition

$$\xi_h \sqrt{\frac{m}{\hbar t}} \frac{\mu}{\hbar\omega_\perp} \ll 1, \quad (41)$$

which easily holds for the parameters shown in Figs. 1 and 2. In addition, one can use Feshbach resonances [44] to completely switch off interactions during the expansion.

Locally, corrections due to finite L can be neglected, if finite limits of integration in Eq. (16) lead to smearing of delta-functions up to the distances at which the correlation functions change considerably. This change can

occur either because of the variations of the density in external confinement at distances $\sim L$, or because of the decay of correlations for finite temperatures at distances of the order $\sim K\xi_h/a$. Thus for finite temperatures these conditions read

$$\frac{mL}{\hbar t} \min(L, K\xi_h/a) \gg 1, \quad (42)$$

and are easily satisfied for parameters considered earlier, and e.g. longitudinal frequency $\omega_x = 2\pi \times 5$ Hz. Under condition (42) one can take the inhomogeneity of the density profile into account within the local density approximation by averaging the prediction of Eq. (37).

B. Strongly interacting 1D Bose gases

Let us now describe the evolution of the two-point density correlation function $g_2(x; t)$ of a strongly interacting 1D Bose gas. A dimensionless parameter which controls the strength of interactions at zero temperature can be written as

$$\gamma = \frac{mg_{1D}}{\hbar^2 n_{1D}} = \frac{2m\omega_\perp a_s}{\hbar n_{1D}} \gg 1. \quad (43)$$

Under such conditions, the bosonic wave function gets "fermionized", and the density correlation function in the trap $g_2(x; 0)$ is the same as for non-interacting fermions of the same density and temperature. In particular, it vanishes at $x = 0$, and one has $g_2(0; 0) = 0$. However, the correlation functions that contain creation and annihilation operators at different points, such as $\varrho(x_1; x_2; 0)$ in Eq. (20), are not the same as for non-interacting fermions. This happens because bosonic operators, when written in terms of fermionic operators, contain a "string" which ensures proper commutation relations.

In Appendix A we derive a representation of $\varrho(x_1; x_2; 0)$ as a Fredholm-type determinant, which can be easily evaluated numerically. Combining this representation with Eq. (20), we evaluate $g_2(x; t)$ after various expansion times numerically. The results for zero temperature are shown in Fig. 3, while the results for finite temperature $k_B T = \mu \approx 1.2 \frac{(\pi\hbar n_{1D})^2}{2m}$ are shown in Fig. 4. In spite of a considerable change in the temperature, there is no qualitative change in the behavior of $g_2(x; t)$. The qualitative behavior of $g_2(x; t)$ in Figs. 3 and 4 is in agreement with Eq. (44) below, and $\lambda_C \sim n_{1D}^{-1}$ for the Tonks-Girardeau gas.

C. General remarks about 1D case

Before concluding this section we would like to provide a qualitative analysis of the evolution the density correlation function $g_2(x; t)$ as a function of the expansion time t .

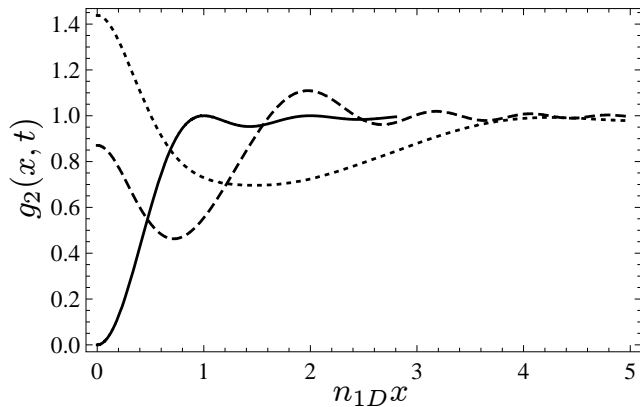


FIG. 3: Two-point density correlation function $g_2(x; t)$ of a zero-temperature strongly interacting 1D Bose gas (Tonks-Girardeau limit) for different times t after the release of the gas from the trap. Different curves correspond to $t = 0$ (solid), $t = 0.25m/(\hbar n_{1D}^2)$ (dashed), and $t = m/(\hbar n_{1D}^2)$ (dotted).

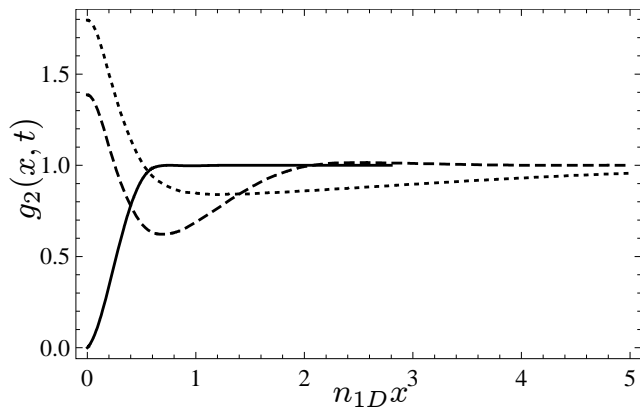


FIG. 4: Two-point density correlation function $g_2(x; t)$ for the same parameters as in Fig. 3, but for a finite temperature, $k_B T = \mu \approx 1.2 \frac{(\pi \hbar n_{1D})^2}{2m}$.

The general structure of the two-particle density matrix $\varrho(x_1; x_2; 0)$ of a 1D Bose gas is shown schematically in Fig. 5. Because of the Bose symmetry, $\varrho(x_1; x_2; 0)$ is represented in the (x_1, x_2) -plane by two infinite perpendicular "bands" of a typical transverse size λ_C (correlation length). For the weakly interacting 1D Bose gas, thermal length λ_T in Eq. (35) plays the role of the correlation length, while for the strongly interacting Tonks-Girardeau regime $\lambda_C \sim n_{1D}^{-1}$. Asymptotically, as $x_1 \rightarrow \pm\infty$ and $x_2 = \pm x_1$, $\varrho \rightarrow n_{1D}^2$. There are several possible cases of atomic correlations near the point $x_1 = x_2 = 0$ in a trapped 1D gas. In general, at $t = 0$, we have $\varrho(0; 0; 0) = n_{1D}^2 g_2(0; 0)$. In the case of the Tonks-Girardeau gas of impenetrable bosons [40, 71] $g_2(0; 0) \equiv g_2^{TG}(0) = 0$ (at zero temperature

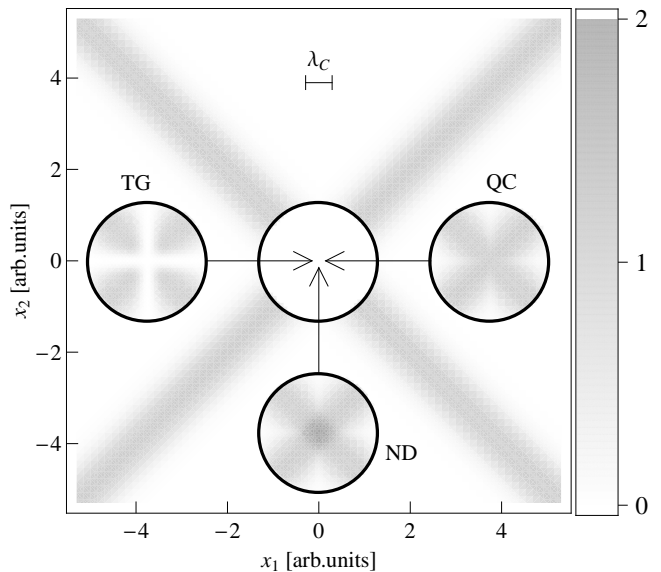


FIG. 5: Density plot of the two-particle density matrix $\varrho(x_1; x_2; 0)$ of a 1D Bose gas, see Eqs. (11) and (17) (the density bar represents the ϱ scale in units of n_{1D}^2). Initially (at $t = 0$) the bosonic system can be a Tonks-Girardeau gas (TG), or a weakly interacting quasicondensate (QC), or a non-degenerate, thermal gas (ND). The central ($x_1 \approx x_2 \approx 0$) part of the two-particle density matrix in these cases is shown in three respective insets. The bar shows the typical correlation scale λ_C .

$g_2^{TG}(x) = 1 - [\sin(\pi n_{1D}x)/(\pi n_{1D}x)]^2$ [40]). Another possibility is a weakly interacting degenerate gas (quasicondensate), where $g_2(0; 0) \equiv g_2^{QC}(0) \approx 1$ [63, 73, 80, 83, 84]. Finally, the 1D Bose gas can be non-degenerate (thermal), in which case $g_2(0; 0) \equiv g_2^{ND} = 2$. As the interparticle distance grows, the density correlation function quite rapidly approaches its asymptotic value $g_2(x \rightarrow \infty; 0) = 1$ at the distances of the order of λ_C .

One can show that time-dependent density correlation function can be written as

$$g_2(x; t) = 1 + \kappa(\lambda_C, x, t) + [g_2(0; 0) - 1]h(\lambda_C, x, t). \quad (44)$$

The first term (unity) stems from the "band" of non-zero values of ϱ aligned along the line $x_1 = x_2$ (see Fig. 5). It represents the density correlation function of an ideal gas of distinguishable particles at equilibrium. The second term, $\kappa(\lambda_C, x, t)$, reflects the Bose-Einstein statistics of the atoms and appears due to the second "band" along $x_2 = -x_1$. Its maximum value, $\kappa(\lambda_C, 0, t)$, increases from 0 to 1 on a typical time scale $\sim m\lambda_C^2/\hbar$. As $|x|$ grows, this term asymptotically approaches 0 on a length scale given by λ_C . The third term describes washing-out of initial short-range (microscopic) correlations. The maximum value of $h(\lambda_C, x, t)$ is reached at $x = 0$, it decreases from 1 to 0 on a time scale $\sim m\lambda_C^2/\hbar$, and $h(\lambda_C, x, t) \approx 0$ if $|x| \gg \lambda_C$. In the course of free evolution, the density correlation properties of an expanding Bose gas become

similar to that of an ideal Bose gas at temperature $k_B T \sim \hbar^2/(m\lambda_C^2)$.

IV. 2D BOSE GASES BELOW THE BEREZINSKII-KOSTERLITZ-THOULESS TEMPERATURE

Let us now discuss the properties of density ripples in expanding 2D clouds. Recently 2D condensates have been realized experimentally in several groups [8, 15, 54, 85, 86, 88]. Reduced dimensionality has dramatic effect on thermal fluctuations. In the case of 2D Bose gases there is no true long-range order for any finite temperature [45]. For uniform 2D Bose clouds at sufficiently low temperatures, the two-point correlation function behaves at large distances as [61, 70, 89, 90]

$$\langle \hat{\psi}^\dagger(\mathbf{r}, 0) \hat{\psi}(0, 0) \rangle \approx n_{2D} \left(\frac{\lambda_{2D}}{r} \right)^\eta \text{ for } r \gg \lambda_{2D}. \quad (45)$$

For the weakly interacting 2D Bose gas at small temperatures, one can evaluate parameters of Eq. (45) from microscopic theory. The dimensionless parameter characterizing weakness of interactions is written as [70, 90]

$$\tilde{g} = a_s \sqrt{\frac{8\pi m \omega_\perp}{\hbar}} \ll 1. \quad (46)$$

The exponent η in Eq. (45) equals [70, 90]

$$\eta = \frac{T}{T_d} \ll 1 \text{ for } k_B T \ll k_B T_d = \frac{2\pi\hbar^2 n_{2D}}{m}, \quad (47)$$

and λ_{2D} equals the de Broglie wavelength of thermal phonons $\hbar c/(k_B T)$ at $k_B T \ll \mu$, and the two-dimensional healing length $\xi_{2D} = \hbar/\sqrt{m\mu}$ at high temperatures $k_B T \gg \mu$.

Equation (45) remains valid for η smaller than

$$\eta_c = 1/4, \quad (48)$$

at which point the BKT [6, 7, 103] transition takes place due to proliferation of vortices, and correlation functions start to decay exponentially with distance.

Such a transition for ultra cold 2D Bose gases has been observed recently [8, 54, 88], and its microscopic origin has been elucidated. This experiment studied interference of two independent 2D Bose clouds, which requires imaging along the "in-plane" direction and inevitably leads to averaging over inhomogeneous densities. Study of the spectrum of density ripples in expanding clouds with imaging in transverse direction (as done in Ref. [54]) avoids this problem altogether, and can provide access to properties of correlations at fixed density. The interplay between the BKT transition and the effects of the external confinement is a rather complicated question even for weakly interacting Bose gas [86, 87, 91, 92], and we will only discuss the uniform case here.

Even for weak interactions, one cannot use quasicondensate theory to analytically describe correlations as functions of microscopic parameters in the vicinity of the BKT transition or to predict the transition temperature, and has to resort to fully numerical methods [93]. Nevertheless, the factorization property (25) remains valid for large-distance behavior of correlation functions for all η below the critical value 1/4, since large-distance fluctuations of the phase are still described by the Gaussian theory. Using that together with Eq. (45), we will now obtain the prediction for the spectrum of density ripples which is valid as long as only points with relative distances much larger than λ_{2D} contribute significantly to the integral in Eq. (23). We will show below, that this regime is realized if

$$\sqrt{\frac{\hbar t}{m}} \gg \lambda_{2D}. \quad (49)$$

We introduce a dimensionless variable

$$y = \frac{\hbar q^2 t}{m}, \quad (50)$$

and use expression Eq. (45) for all \mathbf{r} . Using symmetries of the resulting integral, the expression for $\langle |\rho(q, t)|^2 \rangle$ is written as

$$\langle |\rho(q, t)|^2 \rangle \approx n_{2D}^2 \lambda_{2D}^2 \left(\frac{\hbar t}{m \lambda_{2D}^2} \right)^{1-\eta} F(\eta, y), \quad (51)$$

where $F(\eta, y)$ is a dimensionless function defined by [108]

$$F(\eta, y) = \frac{4}{y^{1+\eta}} \int_0^\infty dr_x \cos r_x \int_0^\infty dr_y \left\{ \left[\frac{\sqrt{(r_x + y)^2 + r_y^2} \sqrt{(r_x - y)^2 + r_y^2}}{r_x^2 + r_y^2} \right]^\eta - 1 \right\}. \quad (52)$$

We find that the spectrum of density ripples remains self-similar in the course of expansion and the shape of the spectrum is a function of η only. Plots of $F(\eta, y)$ for three different values of η are shown in Fig. 6, and have a similar structure. Positions of maxima and minima are very well described by Eq. (39), where the upper (lower) sign corresponds to the n -th maximum (minimum). In Eq. (23) typical distances which contribute to $\langle |\rho(q, t)|^2 \rangle$ near its maximum at $y \approx \pi$ can be estimated as $\sim \sqrt{\hbar t/m}$, which leads to condition (49). Note however, that self-similarity starts breaking down for sufficiently large y even when condition (49) is satisfied.

Scaling of the magnitude of $\langle |\rho(q, t)|^2 \rangle$ with time in the self-similar regime can be used to extract η . For example, the integral of $\langle |\rho(q, t)|^2 \rangle$ from 0 to its first minimum scales with time as

$$\int_0^{\sqrt{\frac{2\pi m}{\hbar t}}} dq \langle |\rho(q, t)|^2 \rangle \propto t^{1/2-\eta}, \quad (53)$$

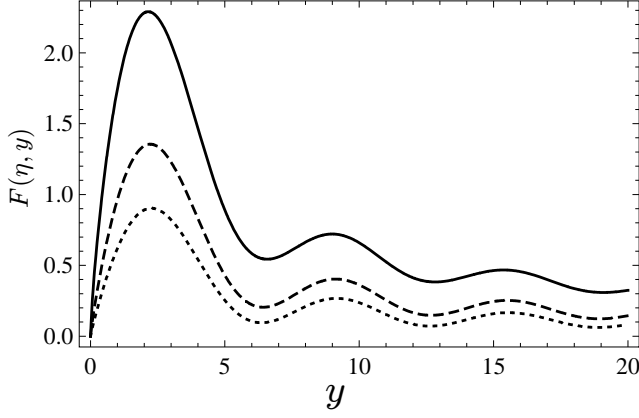


FIG. 6: Dependence of universal functions $F(\eta, y)$ on $y = \frac{\hbar q^2 t}{m}$ plotted for three different values of correlation exponents η . Under condition (49) functions $F(\eta, y)$ determine the self-similar shape of the spectrum of density ripples according to Eq. (51). Curves from top to bottom correspond to $\eta = 0.25$ (solid, the Berezinskii-Kosterlitz-Thouless point), $\eta = 0.15$ (dashed) and $\eta = 0.10$ (dotted).

and the exponent changes considerably as η changes from 0 to the critical value $1/4$.

For small η , one can derive an expansion of $F(\eta, y)$ as

$$F(\eta, y) = \frac{4}{y^{1+\eta}} [\eta f_1(y) + \eta^2 f_2(y) + \eta^3 f_3(y) + \dots], \quad (54)$$

where $f_1(y)$ can be evaluated analytically as

$$f_1(y) = 2\pi \sin^2 \frac{y}{2}. \quad (55)$$

The term $f_2(y)$ leads to a finite value of $F(\eta, y)$ at the first minimum. By including effects of $f_2(y)$ and $f_3(y)$, one can derive

$$\frac{F(\eta, 2\pi)}{F(\eta, \pi)} \approx \frac{1}{2^\eta} (1.19\eta + 0.38\eta^2) \text{ for } \eta \ll 1, \quad (56)$$

which coincides with the direct numerical evaluation up to 2.5% for $\eta = 0.25$.

For weakly interacting uniform 2D Bose gases at low temperatures, one can also obtain predictions which are not limited by Eq. (49). Under condition

$$n_{2D} \xi_{2D}^2 \gg 1 \quad (57)$$

an extension of Bogoliubov theory to 2D quasicondensates describes correlations at all distances [63]. Such a theory is valid up to temperatures of the order

$$\frac{k_B T}{\mu} \log \frac{k_B T}{\mu} \sim n_{2D} \xi_{2D}^2 \gg 1, \quad (58)$$

and predicts the exponent (47). The correlation function is written as

$$g_1(\mathbf{r}) = \frac{\langle \hat{\psi}^\dagger(\mathbf{r}, 0) \hat{\psi}(0, 0) \rangle}{n_{2D}} = \exp \left[-\frac{2\pi\mu}{k_B T_d} f_{2D} \left(\frac{r}{\xi_{2D}} \right) \right],$$

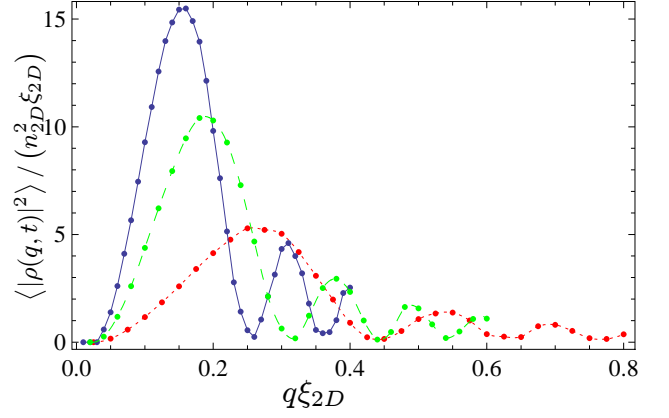


FIG. 7: (Color Online) Normalized spectrum of density ripples $\langle |\rho(q, t)|^2 \rangle / (n_{2D}^2 \xi_{2D})$ for weakly interacting 2D quasicondensate of ^{87}Rb atoms with density $n_{2D} \approx 84 \mu\text{m}^{-2}$, transverse confinement frequency $\omega_\perp = 2\pi \times 3 \text{ kHz}$, healing length $\xi_h \approx 0.3 \mu\text{m}$, and dimensionless interaction parameter $\tilde{g} \approx 0.13$. Temperature is taken to be $T = 60 \text{ nK}$ ($k_B T \approx \mu$), which corresponds to correlation exponent $\eta = 0.020$. Various curves correspond to expansion times $t = 12 \text{ ms}$ (blue, solid), $t = 8 \text{ ms}$ (green, dashed), and $t = 4 \text{ ms}$ (red, dotted). The lines are guides to the eye.

where the dimensionless function $f_{2D}(s)$ is defined by

$$f_{2D}(s) = \int_0^\infty \frac{k dk}{2\pi} [1 - J_0(ks)] \{ [u_k^2 + v_k^2] n_k + v_k^2 \}.$$

Here, $J_0(x)$ is the Bessel function, and u_k, v_k and n_k are defined by Eqs. (28)-(30).

We now consider a case of ^{87}Rb atoms with transverse confinement frequency $\omega_\perp = 2\pi \times 3 \text{ kHz}$, and density $n_{2D} \approx 84 \mu\text{m}^{-2}$. This yields the dimensionless interaction parameter $\tilde{g} \approx 0.13$, healing length $\xi_h \approx 0.3 \mu\text{m}$, and $n_{2D} \xi_{2D}^2 \approx 7.5$. We perform a numerical integration of Eq. (23) for temperature $T = 60 \text{ nK}$ (which corresponds to correlation exponent 0.02) and various expansion times, and the results are shown in Fig. 7.

Qualitatively, they look similar to the self-similar regime for all times, and one again obtains an oscillating spectrum of density ripples with maxima and minima very well described by Eq. (39). In the weakly interacting regime the ratio of the first maximum to the first minimum for $\langle |\rho(q, t)|^2 \rangle$ is much larger than one, similar to the weakly interacting 1D Bose gas.

V. CONCLUSIONS

To conclude, we calculated the evolution of the two-point density correlation function of an ultra cold atomic Bose gas released from a tight transverse confinement.

For 1D gases in the weakly interacting regime, in a wide range of parameters given by Eq. (33), we analytically

calculated the spectrum of density ripples $\langle |\rho(q, t)|^2 \rangle$. Our results are summarized in Eq. (37) and Figs. 1 and 2. Our analytical theory is also applicable in the quasi-1D regime when $k_B T$ and μ are of the order of transverse confinement frequency $\hbar\omega_\perp$. For expansion times smaller than $6.5m\lambda_T^2/\hbar$, we find that the spectrum of density ripples can have several maxima and minima, and their positions can be estimated using Eq. (39). While positions of maxima and minima are essentially independent of the temperature, their amplitude exhibits strong temperature dependence. For 1D quasicondensates, the density profile in external harmonic confinement depends weakly on the temperature, when the latter is of the order of the chemical potential [63]. The density profile follows the "inverted parabola" shape [64], thus the bimodal density fitting cannot be used to measure temperatures reliably. We propose that our analytical result Eq. (37) can be used for thermometry of one-dimensional systems. Experimental investigation of this question is currently under way, and will be presented in a separate publication [109].

For one-dimensional systems, we also discussed the evolution of the density correlation function in real space, $g_2(x; t)$. For long expansion times we find that the correlation function $g_2(x; t)$ reaches the value 2 at short distances and approaches the value 1 for distances larger than the correlation length, see e.g. Fig. 3 for the Tonks-Girardeau regime.

For 2D Bose gases with temperatures below the Berezinskii-Kosterlitz-Thouless transition and sufficiently long expansion time, we showed that the spectrum of the density ripples evolves in a self-similar way. Our result for this case is given in Eq. (51) and Fig. 6, with positions of maxima and minima determined by Eq. (39). The scaling of the overall magnitude can be used to extract the correlation exponent η , e.g. using Eq. (53).

For more complicated situations, e.g. multicomponent gases, relation (21) and its cross-correlation generalizations can be used as a convenient experimental tool to characterize complex many-body states and their correlations. In addition, it can be used as an experimental tool to investigate non-equilibrium phenomena in low-dimensional gases.

A.I. was supported by DOE Grant No. DE-FG02-08ER46482. I.E.M. acknowledges support through the Lise Meitner program by the FWF, and the INTAS. D.S.P. was supported by ANR Grant 08-BLAN-0165-01 and by the Russian Foundation for Fundamental Research. V.G. was supported by Swiss National Science Foundation. S.M. acknowledges support from the FWF doctoral program CoQuS. T.S. acknowledges support by the FWF program P21080. E.D. was supported by the NSF grant DMR-0705472, DARPA, MURI, and Harvard-MIT CUA. J.S. was supported by the EC and the FWF. We acknowledge useful discussions with A. Aspect, P. Cladé, E. Cornell, J. Dalibard, M. Greiner, Z. Hadzibabic, W. Phillips and G. Shlyapnikov.

APPENDIX A: TWO-PARTICLE DENSITY MATRIX OF A STRONGLY INTERACTING 1D BOSE GAS

In this Appendix we will describe a Fredholm-type determinant representation for $\varrho(x_1; x_2; 0)$ for $0 < x_1 < x_2$, which can be easily evaluated numerically. Due to Eqs. (18),(19) this defines $\varrho(x_1; x_2; 0)$ for any values of x_1 and x_2 . Representations similar to the one developed here can be obtained for any multi-point correlation function of bosonic fields in the strongly interacting limit.

Mathematically, "fermionization" can be written as

$$\hat{\psi}^\dagger(x) = \exp \left[i\pi \int_{-\infty}^{x-0} dy \hat{\psi}_f^\dagger(y) \hat{\psi}_f(y) \right] \hat{\psi}_f^\dagger(x), \quad (\text{A1})$$

$$\hat{\psi}(x) = \exp \left[-i\pi \int_{-\infty}^{x-0} dy \hat{\psi}_f^\dagger(y) \hat{\psi}_f(y) \right] \hat{\psi}_f(x), \quad (\text{A2})$$

where we introduced fermionic creation and annihilation operators $\hat{\psi}_f^\dagger(x)$ and $\hat{\psi}_f(x)$, which have standard anti-commutation relations

$$\left\{ \hat{\psi}_f^\dagger(x), \hat{\psi}_f(y) \right\} = \delta(x - y), \quad (\text{A3})$$

$$\left\{ \hat{\psi}_f^\dagger(x), \hat{\psi}_f^\dagger(y) \right\} = \left\{ \hat{\psi}_f(x), \hat{\psi}_f(y) \right\} = 0. \quad (\text{A4})$$

For zero temperature, ground state for fermions corresponds to a filled Fermi sea, whereas at finite temperature one should use a thermal density matrix for non-interacting fermions.

For convenience, we will introduce a fictitious underlying lattice of spacing $a \ll x_1, x_2$, such that

$$\frac{x_1}{2} \frac{1}{a} = m_1 \gg 1, \quad (\text{A5})$$

$$\frac{x_2}{2} \frac{1}{a} = m_2 > m_1 \gg 1, \quad (\text{A6})$$

where m_1 and m_2 are large positive integer numbers. At the end of the calculation, we will take the limit $a \rightarrow 0$ such that $m_1 a \rightarrow x_1/2, m_2 a \rightarrow x_2/2$. On a lattice, "fermionization" rules (A1),(A2) and commutation relations (A3),(A4) are written as

$$\hat{\psi}^\dagger(i) = \prod_{k < i} \left[1 - 2\hat{\psi}_f^\dagger(k) \hat{\psi}_f(k) \right] \hat{\psi}_f^\dagger(i), \quad (\text{A7})$$

$$\hat{\psi}(i) = \prod_{k < i} \left[1 - 2\hat{\psi}_f^\dagger(k) \hat{\psi}_f(k) \right] \hat{\psi}_f(i), \quad (\text{A8})$$

$$\left\{ \hat{\psi}_f^\dagger(i), \hat{\psi}_f(k) \right\} = \delta_{ik}, \quad (\text{A9})$$

$$\left\{ \hat{\psi}_f^\dagger(i), \hat{\psi}_f^\dagger(k) \right\} = \left\{ \hat{\psi}_f(i), \hat{\psi}_f(k) \right\} = 0. \quad (\text{A10})$$

Using these relations, $\varrho(x_1; x_2; 0)$ can be written as

$$\begin{aligned} \varrho(x_1; x_2; 0) &= \left\langle \hat{\psi}_f^\dagger(m_1) \hat{\psi}_f^\dagger(-m_1) \right. \\ &\times \left. \prod_{k \in S} \left[1 - 2\hat{\psi}_f^\dagger(k) \hat{\psi}_f(k) \right] \hat{\psi}_f(m_2) \hat{\psi}_f(-m_2) \right\rangle, \quad (\text{A11}) \end{aligned}$$

where subset S equals

$$S = [-m_2 + 1, -m_1 - 1] \cup [m_1 + 1, m_2 - 1]. \quad (\text{A12})$$

Expanding the parentheses, we obtain

$$\begin{aligned} \varrho(x_1; x_2; 0) = & \left\langle \sum_{n=0}^{\infty} (-2)^n \hat{\psi}_f^\dagger(m_1) \hat{\psi}_f^\dagger(-m_1) \right. \\ & \times \sum_{j_1 < \dots < j_n, j_k \in S} \hat{\psi}_f^\dagger(j_1) \dots \hat{\psi}_f^\dagger(j_n) \hat{\psi}_f(j_n) \dots \hat{\psi}_f(j_1) \\ & \left. \times \hat{\psi}_f(m_2) \hat{\psi}_f(-m_2) \right\rangle. \quad (\text{A13}) \end{aligned}$$

For each n and set of j_1, \dots, j_n , expectation value of $n+2$ creation and $n+2$ annihilation operators can be written using Wick's theorem [110] as a determinant of $(n+2) \times (n+2)$ matrix [111, 112]

$$M_{i,j}^{(n+2)} = aG(s_i, t_j), \quad (\text{A14})$$

where

$$s_1 = -m_1 a, \quad s_2 = m_1 a, \quad s_{i>2} = j_{i-2} a, \quad (\text{A15})$$

$$t_1 = m_2 a, \quad t_2 = -m_2 a, \quad t_{i>2} = j_{i-2} a, \quad (\text{A16})$$

and $G(x, y) = G(x - y)$ is a Green's function of a free Fermi gas, which e.g. for zero temperature equals

$$G(x) = \int_{-k_f}^{k_f} \exp[ikx] \frac{dk}{2\pi} = \frac{\sin \pi n_1 D x}{\pi x}. \quad (\text{A17})$$

Since the structure of the matrix $M_{i,j}^{(n+2)}$ doesn't depend on n , summation over different n and sets j_1, \dots, j_n can be now represented as a single Fredholm-type determinant [112, 113]

$$\varrho(x_1; x_2; 0) = \frac{\text{Det} [A_{ij} - 2aB_{ij}]}{4a^2}, \quad (\text{A18})$$

where matrices A_{ij} and B_{ij} of size $2(m_2 - m_1) \times 2(m_2 - m_1)$ are defined by

$$A_{ij} = \text{Diag}\{0, 0, 1, \dots, 1\}, \quad (\text{A19})$$

$$B_{ij} = G(\tilde{s}_i, \tilde{t}_j), \quad (\text{A20})$$

and

$$\tilde{s}_1 = -m_1 a, \quad \tilde{s}_2 = m_1 a, \quad (\text{A21})$$

$$\tilde{s}_i = (-m_2 + i - 2) a \text{ for } 3 \leq i < 2 + m_2 - m_1, \quad (\text{A22})$$

$$\tilde{s}_i = (2m_1 - m_2 + i - 1) a \text{ for}$$

$$2 + m_2 - m_1 \leq i \leq 2(m_2 - m_1), \quad (\text{A23})$$

$$\tilde{t}_1 = m_2 a, \quad \tilde{t}_2 = -m_2 a, \quad \tilde{t}_{i>2} = \tilde{s}_i. \quad (\text{A24})$$

Expansion of the determinant of $A_{ij} - 2aB_{ij}$ using the rule for the determinant of the sum of two matrices (see e.g. p. 221 of Ref. [114]) generates the expansion of Eq. (A13), similar to a usual Fredholm determinant [113]. Indeed, only diagonal minors not including lines 1 and 2 can be chosen from the matrix A_{ij} . Complimentary minor of size $(n+2) \times (n+2)$ from the matrix B_{ij} is proportional to matrix $M^{(n+2)}$ in Eq. (A14), and the summation over possible different sets of j_1, \dots, j_n is equivalent to a summation over different partitions of matrix A_{ij} into diagonal minors.

Since determinants are easy to evaluate numerically, one can now take the limit $a \rightarrow 0$ numerically and evaluate $\varrho(x_1; x_2; 0)$ with any precision.

-
- [1] M. Greiner *et al.*, Nature (London) **415**, 39 (2002).
 - [2] U. Schneider *et al.*, Science **322**, 1520 (2008).
 - [3] A. Perrin *et al.*, Phys. Rev. Lett. **99**, 150405 (2007).
 - [4] S. Hofferberth *et al.*, Nature (London) **449**, 324 (2007).
 - [5] S. Hofferberth *et al.*, Nat. Phys. **4**, 489 (2008).
 - [6] V. L. Berezinskii, Sov. Phys. JETP **32**, 493 (1971); *ibid.* **34**, 610 (1972).
 - [7] J. M. Kosterlitz and D. J. Thouless, J. Phys. C **6**, 1181 (1973); J. M. Kosterlitz, J. Phys. C **7**, 1046 (1974).
 - [8] Z. Hadzibabic *et al.*, Nature (London) **441**, 1118 (2006).
 - [9] M. Schellekens *et al.*, Science **310**, 648 (2005).
 - [10] T. Jelts *et al.*, Nature (London) **445**, 402 (2007).
 - [11] S. Fölling *et al.*, Nature (London) **434**, 481 (2005).
 - [12] T. Rom *et al.*, Nature (London) **444**, 733 (2006).
 - [13] A. Öttl, S. Ritter, M. Köhl, and T. Esslinger, Phys. Rev. Lett. **95**, 090404 (2005).
 - [14] F. Schreck *et al.*, Phys. Rev. Lett. **87**, 080403 (2001).
 - [15] A. Görlitz *et al.*, Phys. Rev. Lett. **87**, 130402 (2001).
 - [16] T. Kinoshita, T. Wenger, and D. S. Weiss, Science **305**, 1125 (2004).
 - [17] B. Paredes *et al.*, Nature (London) **429**, 277 (2004).
 - [18] T. Kinoshita, T. Wenger, and D. S. Weiss, Phys. Rev. Lett. **95**, 190406 (2005).
 - [19] B. Laburthe Tolra *et al.*, Phys. Rev. Lett. **92**, 190401 (2004).
 - [20] Yu. Kagan, B. V. Svistunov, and G. V. Shlyapnikov, JETP Lett. **42**, 209 (1985).
 - [21] Y. Miroshnychenko, W. Alt, I. Dotsenko, L. Förster, D. Meschede, D. Schrader, M. Khudaverdyan, and A. Rauschenbeutel, Nature (London) **442**, 151 (2006).
 - [22] Y. Colombe, T. Steinmetz, G. Dubois, F. Linke, D. Hunger, and J. Reichel, Nature (London) **450**, 272 (2007).
 - [23] K. D. Nelson, X. Li, and D. S. Weiss, Nat. Phys. **3**, 556

- (2007).
- [24] T. Gericke, P. Würtz, D. Reitz, T. Langen, and H. Ott, *Nat. Phys.* **4**, 949 (2008).
- [25] M. Wilzbach *et al.*, *Opt. Lett.* **34**, 259 (2009).
- [26] D. Heine *et al.*, *Phys. Rev. A* **79**, 021804(R) (2009).
- [27] D. S. Petrov, G. V. Shlyapnikov, and J. T. M. Walraven, *Phys. Rev. Lett.* **87**, 050404 (2001).
- [28] S. Dettmer *et al.*, *Phys. Rev. Lett.* **87**, 160406 (2001).
- [29] D. Hellweg *et al.*, *Appl. Phys. B* **73**, 781 (2001).
- [30] H. Kreutzmann *et al.*, *Appl. Phys. B* **76**, 165 (2003)
- [31] P. Öhberg and L. Santos, *Phys. Rev. Lett.* **89**, 240402 (2002); P. Pedri, L. Santos, P. Öhberg, and S. Stringari, *Phys. Rev. A* **68**, 043601 (2003).
- [32] M. Rigol and A. Muramatsu, *Phys. Rev. Lett.* **93**, 230404 (2004); *ibid.* **94**, 240403 (2005); *Mod. Phys. Lett. B* **19**, 861 (2005).
- [33] A. Minguzzi and D. M. Gangardt, *Phys. Rev. Lett* **94**, 240404 (2005).
- [34] M. Rigol, V. Dunjko, V. Yurovsky, and M. Olshanii, *Phys. Rev. Lett.* **98**, 050405 (2007).
- [35] D. M. Gangardt and M. Pustilnik, *Phys. Rev. A* **77**, 041604(R) (2008).
- [36] H. Buljan, R. Pezer, and T. Gasenzer, *Phys. Rev. Lett.* **100**, 080406 (2008); *ibid.* **102**, 049903(E) (2009).
- [37] D. Jukić, R. Pezer, T. Gasenzer, and H. Buljan, *Phys. Rev. A* **78**, 053602 (2008).
- [38] D. Jukić, B. Klajn, and H. Buljan, *Phys. Rev. A* **79**, 033612 (2009).
- [39] A. del Campo and J. G. Muga, *Europhys. Lett.* **74**, 965 (2006).
- [40] M. Girardeau, *J. Math. Phys.* **1**, 516 (1960).
- [41] N. Bogoliubov, *J. Phys. (Moscow)* **11**, 23 (1947).
- [42] L. Pitaevskii and S. Stringari, *Bose-Einstein condensation* (Oxford Science Publishing, Oxford, 2003).
- [43] C. J. Pethick and H. Smith, *Bose-Einstein Condensation in Dilute Gases* (Cambridge University Press, Cambridge, England, 2001).
- [44] S. Inouye *et al.*, *Nature (London)* **392**, 151 (1998); P. Courteille *et al.*, *Phys. Rev. Lett.* **81**, 69 (1998); J. L. Roberts *et al.*, *ibid.* **81**, 5109 (1998).
- [45] N. D. Mermin and H. Wagner, *Phys. Rev. Lett.* **17**, 1133 (1966); P. C. Hohenberg, *Phys. Rev.* **158**, 383 (1967).
- [46] S. Coleman, *Commun. Math. Phys.* **31**, 259 (1973).
- [47] P. D. Naselsky, D. I. Novikov, and I. D. Novikov, *The Physics of the Cosmic Microwave Background* (Cambridge University Press, Cambridge, England, 2006).
- [48] J. C. Mather, *Rev. Mod. Phys.* **79**, 1331 (2007); G. F. Smoot, *ibid.* **79**, 1349 (2007).
- [49] T. Padmanabhan, *Structure formation in the universe* (Cambridge University Press, Cambridge, England, 1993).
- [50] D. Hellweg *et al.*, *Phys. Rev. Lett.* **91**, 010406 (2003); L. Cacciapuoti *et al.*, *Phys. Rev. A* **68**, 053612 (2003).
- [51] F. Gerbier *et al.*, *Phys. Rev. A* **67**, 051602(R) (2003).
- [52] S. Richard *et al.*, *Phys. Rev. Lett.* **91**, 010405 (2003).
- [53] M. Hugbart *et al.*, *Eur. Phys. J. D* **35**, 155 (2005).
- [54] P. Cladé, C. Ryu, A. Ramanathan, K. Helmerson, and W. D. Phillips, *Phys. Rev. Lett.* **102**, 170401 (2009).
- [55] E. Altman, E. Demler, and M. D. Lukin, *Phys. Rev. A* **70**, 013603 (2004).
- [56] J. Esteve *et al.*, *Phys. Rev. Lett.* **96**, 130403 (2006).
- [57] A. Polkovnikov, E. Altman, and E. Demler, *Proc. Natl. Acad. Sci. U.S.A.* **103**, 6125 (2006).
- [58] V. Gritsev, E. Altman, E. Demler, and A. Polkovnikov, *Nat. Phys.* **2**, 705 (2006).
- [59] A. Imambekov, V. Gritsev, and E. Demler, *Phys. Rev. A* **77**, 063606 (2008).
- [60] A. Imambekov, V. Gritsev, and E. Demler, in *Ultra-Cold Fermi Gases*, Proceedings of the International School of Physics "Enrico Fermi," 2006 (IOS Press, 2006); arXiv:cond-mat/0703766v1.
- [61] V. N. Popov, *Theor. Math. Phys.* **11**, 565 (1972); *Functional Integrals in Quantum Field Theory and Statistical Physics* (Reidel, Dordrecht, 1983).
- [62] D. S. Petrov, G. V. Shlyapnikov, and J. T. M. Walraven, *Phys. Rev. Lett.* **85**, 3745 (2000).
- [63] C. Mora and Y. Castin, *Phys. Rev. A* **57**, 053615 (2003); Y. Castin, *J. Phys. IV* **116**, 89 (2004).
- [64] C. Gils, L. Pollet, A. Vernier, F. Hebert, G. G. Batrouni, and M. Troyer, *Phys. Rev. A* **75**, 063631 (2007).
- [65] K. B. Efetov and A. I. Larkin, *Sov. Phys. JETP* **42**, 390 (1975).
- [66] F. D. M. Haldane, *Phys. Rev. Lett.* **47**, 1840 (1981).
- [67] M. A. Cazalilla, *J. Phys. B* **37**, S1 (2004).
- [68] J. O. Andersen, U. Al Khawaja, and H. T. C. Stoof, *Phys. Rev. Lett.* **88**, 070407 (2002).
- [69] U. Al Khawaja, J. O. Andersen, N. P. Proukakis, and H. T. C. Stoof, *Phys. Rev. A* **66**, 013615 (2002).
- [70] D. S. Petrov, D. M. Gangardt, and G. V. Shlyapnikov, *J. Phys. IV* **116**, 5 (2004).
- [71] A. Lenard, *J. Math. Phys.* **5**, 930 (1964); H. G. Vaidya and C. A. Tracy, *Phys. Rev. Lett.* **42**, 3 (1979); **43**, 1540 (1979).
- [72] E. H. Lieb and W. Liniger, *Phys. Rev.* **130**, 1605 (1963); E. H. Lieb, *ibid.* **130**, 1616 (1963).
- [73] D. M. Gangardt and G. V. Shlyapnikov, *Phys. Rev. Lett.* **90**, 010401 (2003); D. M. Gangardt and G. V. Shlyapnikov, *New J. Phys.* **5**, 79 (2003); K. V. Kheruntsyan, D. M. Gangardt, P. D. Drummond, and G. V. Shlyapnikov, *Phys. Rev. Lett.* **91**, 040403 (2003).
- [74] V. V. Cheianov, H. Smith, and M. B. Zvonarev, *Phys. Rev. A* **73**, 051604(R) (2006); *J. Stat. Mech.* P08015 (2006).
- [75] J.-S. Caux and P. Calabrese, *Phys. Rev. A* **74**, 031605(R) (2006).
- [76] J.-S. Caux, P. Calabrese, and N. A. Slavnov, *J. Stat. Mech.* (2007) P01008.
- [77] A. Imambekov and L. I. Glazman, *Phys. Rev. Lett.* **100**, 206805 (2008).
- [78] A. Yu. Cherny and J. Brand, *J. Phys.: Conf. Ser.* **129**, 012051 (2008); *Phys. Rev. A* **79**, 043607 (2009).
- [79] V. Gritsev, T. Rostunov, and E. Demler, arXiv:0904.3221v1.
- [80] G. E. Astrakharchik and S. Giorgini, *Phys. Rev. A* **68**, 031602(R) (2003).
- [81] P. D. Drummond, P. Deuar, and K. V. Kheruntsyan, *Phys. Rev. Lett.* **92**, 040405 (2004).
- [82] I. Bouchoule, K. V. Kheruntsyan, and G. V. Shlyapnikov, *Phys. Rev. A* **75**, 031606(R) (2007).
- [83] A. G. Sykes *et al.*, *Phys. Rev. Lett.* **100**, 160406 (2008).
- [84] P. Deuar *et al.*, *Phys. Rev. A* **79**, 043619 (2009).
- [85] S. Burger *et al.*, *Europhys. Lett.* **57**, 1 (2002); D. Rychtarik, B. Engeser, H.-C. Nägerl, and R. Grimm, *Phys. Rev. Lett.* **92**, 173003 (2004); Z. Hadzibabic, S. Stock, B. Battelier, V. Bretin, and J. Dalibard, *ibid.* **93**, 180403 (2004); N. L. Smith *et al.*, *J. Phys. B* **38**, 223 (2005).

- [86] P. Krüger, Z. Hadzibabic, and J. Dalibard, Phys. Rev. Lett. **99**, 040402 (2007).
- [87] Z. Hadzibabic *et al.*, New J. Phys. **10**, 045006 (2008).
- [88] V. Schweikhard, S. Tung, and E. A. Cornell, Phys. Rev. Lett. **99**, 030401 (2007).
- [89] W. Kane and L. Kadanoff, Phys. Rev. **155**, 80 (1967); J. Math. Phys. **6**, 1902 (1965).
- [90] D. S. Petrov, M. Holtzmann, and G. V. Shlyapnikov, Phys. Rev. Lett. **84**, 2551 (2000).
- [91] A. Posazhennikova, Rev. Mod. Phys. **78**, 1111 (2006).
- [92] M. Holzmann, G. Baym, J.-P. Blaizot, and F. Laloë, Proc. Natl. Acad. Sci. U.S.A. **104**, 1476 (2007); M. Holzmann and W. Krauth, Phys. Rev. Lett. **100**, 190402 (2008); M. Holzmann, M. Chevallier, and W. Krauth, Europhys. Lett. **82**, 30001 (2008).
- [93] N. Prokof'ev, O. Ruebenacker, and B. Svistunov, Phys. Rev. Lett. **87**, 270402 (2001).
- [94] N. Prokof'ev and B. Svistunov, Phys. Rev. A **66**, 043608 (2002).
- [95] J. P. Fernández and W. J. Mullin, J. Low Temp. Phys. **128**, 233 (2002).
- [96] C. Gies and D. A. W. Hutchinson, Phys. Rev. A **70**, 043606 (2004).
- [97] D. A. W. Hutchinson and P. B. Blakie, Int. J. Mod. Phys. B **20**, 5224 (2006).
- [98] R. P. Feynman and A. R. Hibbs, *Quantum Mechanics and Path Integrals* (McGraw-Hill, New York, 1965).
- [99] L. Mathey, E. Altman, and A. Vishwanath, Phys. Rev. Lett. **100**, 240401 (2008); L. Mathey, A. Vishwanath, and E. Altman, Phys. Rev. A **79**, 013609 (2009).
- [100] Note an extra factor $\frac{1}{2}$ in front of the mass in Eq. (16), in contrast to Eq. (10).
- [101] One should note that, strictly speaking, $\langle |\rho(q, t)|^2 \rangle$ does not have to be positive, since it is not an expectation value of a positive operator. Square of the operator $\int dx \exp(iqx) \hat{\psi}^\dagger(x, t) \hat{\psi}(x, t)$ differs from $L \langle |\rho(q, t)|^2 \rangle$ by a term which arises due to normal ordering present in the definition of $g_2(x; t)$.
- [102] In the right hand side of Eq. (22) the term -1 in the parentheses was introduced to compensate for the large distance behavior of $g_2(x; t)$, and does not affect the spectrum at $q \neq 0$.
- [103] A. Gogolin, A. Nersisyan, and A. Tsvelik, *Bosonization and Strongly Correlated Systems* (Cambridge University Press, Cambridge, England, 1998).
- [104] T. Giamarchi, *Quantum Physics in One Dimension* (Oxford University Press, New York, 2004).
- [105] H. F. Talbot, Philos. Mag. **9**, 401 (1836).
- [106] M. S. Chapman, C. R. Ekstrom, T. D. Hammond, J. Schmiedmayer, B. E. Tannian, S. Wehinger, and D. E. Pritchard, Phys. Rev. A **51**, R14 (1995).
- [107] F. Gerbier, Europhys. Lett. **66**, 771 (2004).
- [108] Constant -1 in Eq. (52) is included for the convenience to make the integrand vanish at $r_y \rightarrow \infty$, and its contribution disappears after integration over r_x .
- [109] S. Manz *et al.*, to be published.
- [110] A. A. Abrikosov, L. P. Gorkov, and I. E. Dzyaloshinski, *Methods of Quantum Field Theory in Statistical Physics*, (Dover, New York, 1963).
- [111] E. Burovski, N. Prokof'ev, B. Svistunov, and M. Troyer, New J. Phys. **8**, 153 (2006).
- [112] M. B. Zvonarev, V. V. Cheianov, and T. Giamarchi, arXiv:0812.4059v1.
- [113] V. I. Smirnov, *A course of higher mathematics*, Vol IV, p. 24 (Pergamon, Oxford, 1964).
- [114] V. E. Korepin, N. M. Bogoliubov, and A. G. Izergin, *Quantum Inverse Scattering Method and Correlation Functions* (Cambridge University Press, Cambridge, England, 1993).